Heliyon

ELSEVIER

Received:
30 November 2016
Revised:
2 February 2017
Accepted:
13 February 2017

Heliyon 3 (2017) e00253

Effect of solvents on morphology, magnetic and dielectric properties of (α-Fe_2O_3@SiO_2) core-shell nanoparticles

Deepika P Joshi [a,*], **Geeta Pant** [a], **Neha Arora** [a], **Seema Nainwal** [b]

[a] *Department of Physics, Govind Ballabh Pant University of Agriculture & Technology, Pantnagar Uttarakhand, India*

[b] *Department of Physics, Uttaranchal College of Bio Medical Science & Hospital, Dehradun, Uttarakhand, India*

* Corresponding author.

E-mail address: deepikakandpal@gmail.com (D.P. Joshi).

Abstract

Present work describes the formation of α-Fe_2O_3@SiO_2 core shell structure by systematic layer by layer deposition of silica shell on core iron oxide nanoparticles prepared via various solvents. Sol-gel method has been used to synthesize magnetic core and the dielectric shell. The average crystallite size of iron oxide nanoparticles was calculated ~20 nm by X-ray diffraction pattern. Morphological study by scanning electron microscopy revealed that the core-shell nanoparticles were spherical in shape and the average size of nanoparticles increased by varying solvent from methanol to ethanol to isopropanol due to different chemical structure and nature of the solvents. It was also observed that the particles prepared by solvent ethanol were more regular and homogeneous as compared to other solvents. Magnetic measurements showed the weak ferromagnetic behaviour of both core α-Fe_2O_3 and silica-coated iron oxide nanoparticles which remained same irrespective of the solvent chosen. However, magnetization showed dependency on the types of solvent chosen due to the variation in shell thickness. At room temperature, dielectric constant and dielectric loss of silica nanoparticles for all the solvents showed decrement with the increment in frequency. Decrement in the value of dielectric constant and increment in dielectric loss was observed for silica

http://dx.doi.org/10.1016/j.heliyon.2017.e00253

coated iron oxide nanoparticles in comparison of pure silica, due to the presence of metallic core. Homogeneous and regular silica layer prepared by using ethanol as a solvent could serve as protecting layer to shield the magnetic behaviour of iron oxide nanoparticles as well as to provide better thermal insulation over pure α-Fe_2O_3 nanoparticles.

Keywords: Engineering, Materials science, Nanotechnology

1. Introduction

As nanoparticles are smaller than bulk material and larger than individual atoms and molecules, therefore they don't follow absolute quantum chemistry and laws of classical physics. It has been seen that many conventional materials change their optical, thermal, magnetic properties, strength and reactivity in nano form because of quantum effect and increased surface area [1, 2, 3]. Currently, different kinds of magnetic nanoparticles [4, 5, 6, 7, 8, 9], nano-composites [10, 11], doped ferrite nanomaterials [12] and materials with nanostructures [13, 14] have been paid much attention concerning their advance properties.

The magnetic nanoparticles made up of elements having magnetic properties, like cobalt, iron, and nickel show immense potential in many fields such as optical fibre, data storage, tissue targeting, biomedical and medicinal fields etc. [15, 16, 17, 18]. They possess the unique property of superparamagnetism due to their very small particle size [19, 20, 21, 22, 23]. Superparamagnetic nanoparticles offer a high potential for several biomedical applications, such as contrast agents in magnetic resonance imaging (MRI), hyperthermia magnetic separation in microbiology and detoxification of biological fluids. Hematite is the most attractive and important phase amongst all phases of iron oxide nano particles. Considering the ambient condition of all iron oxides, it is most stable. It was able to drawn the attention of researchers because of its enhanced properties. Hematite shows different magnetic properties at different temperatures, it shows antiferro-magnetic properties below its Morin transition (T_M) which is around 260 K and weak ferromagnetic behaviour between its Morin transition ($T_{M;\ 260\ K}$) and Neel temperature (T_N; 948 K) [24, 25, 26, 27].

Dielectric properties of nano materials depend on size, shape, composition as well as the way they are fabricated. Information about conduction phenomenon can be gained by studying the influences of frequency and temperature on dielectric properties of nano substances [28, 29, 30, 31, 32]. **S**ilica nanoparticles have gained importance in recent years because of their applications in various areas and easy synthesis process. Surface modification opens up the door for its future application in the field of biotechnology and medicine such as for cancer treatment, dental filling composites and drug delivery [33, 34].

http://dx.doi.org/10.1016/j.heliyon.2017.e00253

Core-Shell nanoparticles are hybrid systems. They have a core and a shell having distinct attributes such as metallicity, semiconductivity, magnetism etc. Core-shell structures are modified in a way that they can protect the core from the chemical environment of the medium. The surface of the nanoparticles plays a major role in modifying their physical, optical and magnetic properties. Hence, the best way to improve the quality of the nanoparticles is to form a shell over core nanoparticles. Creation of such core shell nanoparticles enables us to achieve properties that cannot be achieved with uncoated nanoparticles. Thus, core shell or layered structure of different materials is an efficient way to fabricate systems possessing diverse physical, chemical, optical and magnetic properties [35, 36]. Present study is focused on the effect of different solvents on morphology, magnetic and dielectric properties of silica coated iron oxide core-shell nanoparticles.

2. Materials and methods

The chemicals used in the present experiment were Ferric nitrate ((Fe $(NO_3)_3.9H_2O$, 98%, Sigma Aldrich); Ethylene glycol ($C_2H_6O_2$, 99%, Sigma Aldrich); Tetraethylorthosilicate (TEOS, 99%, Molychem); Ethanol (C_2H_5OH, 99.9%), Methanol (CH_3OH, 99.9%) and Isopropanol (C_3H_7OH, 99.9%, Changshu Yangyuan Chemicals); Ammonium hydroxide (NH_4OH, 29% in water, Himedia). All the chemicals were used as such, without further purification. Deionised water was used in all experiments. The procedure of synthesizing α-Fe_2O_3, pure silica (SiO_2) nanoparticles and α-Fe_2O_3@SiO_2 core-shell nanoparticles is described in following schematic diagram {Fig. 1(a), (b) and (c)} respectively.

3. Result and discussion

3.1. Structural and morphological properties

3.1.1. (a) XRD pattern of iron oxide nanoparticles

The XRD pattern of prepared iron oxide nanoparticles is presented in Fig. 2 Cu-Kα ($\lambda = 1.54$ Å) radiation was used to record the XRD pattern of the prepared samples. The most intense peak was observed at $2\theta = 35.67°$. The diffraction peaks appeared at different angles (2θ) corroborated with the JCPDS-86-0550 values, which can be correlated with the (012), (104), (110), (113), (024), (116), (018), (214) and (300) planes of hematite (α-Fe_2O_3). This revealed that the resultant particles are pure α-Fe_2O_3 without the presence of any other impurities and other forms of iron oxide phases. Broad nature of the diffraction pattern is an indication of the smaller sized particles. The average crystalline size from the most intense peak of the XRD pattern was obtained using Scherrer's formula [37].

http://dx.doi.org/10.1016/j.heliyon.2017.e00253

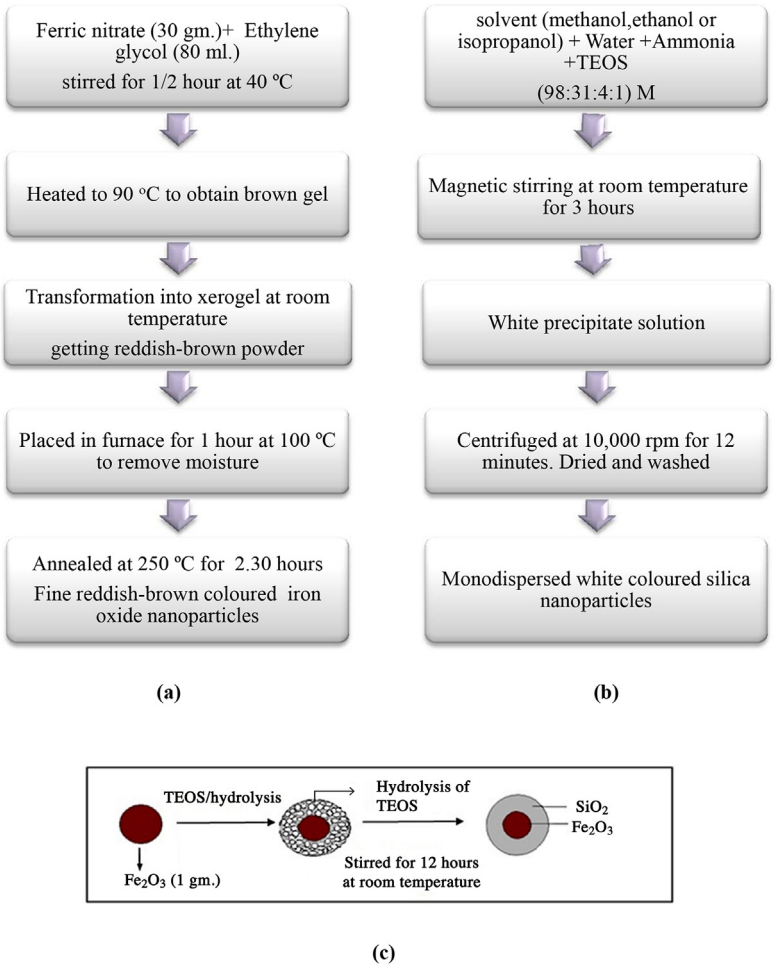

Fig. 1. Schematic representation for synthesis of (a) Iron oxide (b) silica and (c) α-Fe_2O_3@SiO_2 nanoparticles.

$$D = \frac{k\lambda}{\beta\cos(\theta)}$$

Here, λ is the X-ray wavelength ($Cu_{K\alpha}$), k is the machine constant, β is the full width at half maximum (FWHM in radian) of the peak and θ is the peak angle. The shape of the prepared crystal of α-Fe_2O_3 was found hexagonal from JCPDS-86-0550 and average crystalline size was obtained ~20 nm. Lattice parameters of the synthesized α-Fe_2O_3 nanoparticles are tabulated in Table 1.

3.1.2. (b) FT-IR spectra of α-Fe_2O_3@SiO_2core- shell nanoparticles

The FT-IR analysis was performed for the synthesized silica-coated hematite core-shell nanoparticles to confirm the bonding of silica nanoparticle with the α-Fe_2O_3 nanoparticles. The feature functional groups of synthesized α-Fe_2O_3@SiO_2 NPs

http://dx.doi.org/10.1016/j.heliyon.2017.e00253

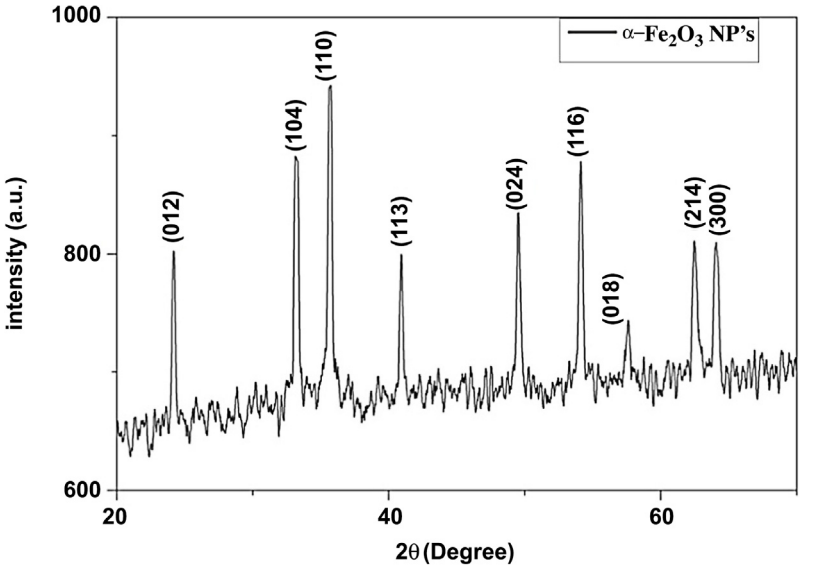

Fig. 2. XRD pattern of Iron oxide nanoparticles.

have been discussed by FTIR analysis in the wave number range of 500–4000 cm^{-1} and graphically shown in Fig. 3.

The peaks at 677 cm^{-1} are due to the vibration of Fe–O bond that matches well with the characteristic peaks of Fe_2O_3. The peak at 1094 cm^{-1} due to Si-O-Fe indicates the presence of silica content on iron oxide. Intensity of the sharp peak assigned to the stretching vibrations of Si–O–Fe bond its intensity increases with the increase of the SiO_2 shell thickness [38, 39]. So, from graphical view also, it is clear that the thickness of silica layer increased with different solvents from methanol to isopropanol. The band at 1653 cm^{-1} is assigned to C═O stretching. The peak at 2956 cm^{-1} corresponds to the C–H stretching of $–CH_2$ groups [40].

The obtained results suggested the strong interactions in the interfaces between the α-Fe_2O_3 cores and SiO_2 shells. These results confirmed that α-Fe_2O_3@SiO_2 nanoparticles were prepared successfully.

3.1.3. (c) SEM analysis

SEM images of silica coated iron oxide core-shell nanoparticles prepared by using methanol, ethanol and isopropanol as solvent are shown in Fig. 4(a), (b) and (c)

Table 1. Crystallographic data obtained from XRD of α-Fe_2O_3.

Sample	Lattice parameters (Å)			Crystallite size (nm)	Shape
	a	*b*	*c*		
α-Fe_2O_3	5.0351	5.0351	13.7483	20	Hexagonal

http://dx.doi.org/10.1016/j.heliyon.2017.e00253

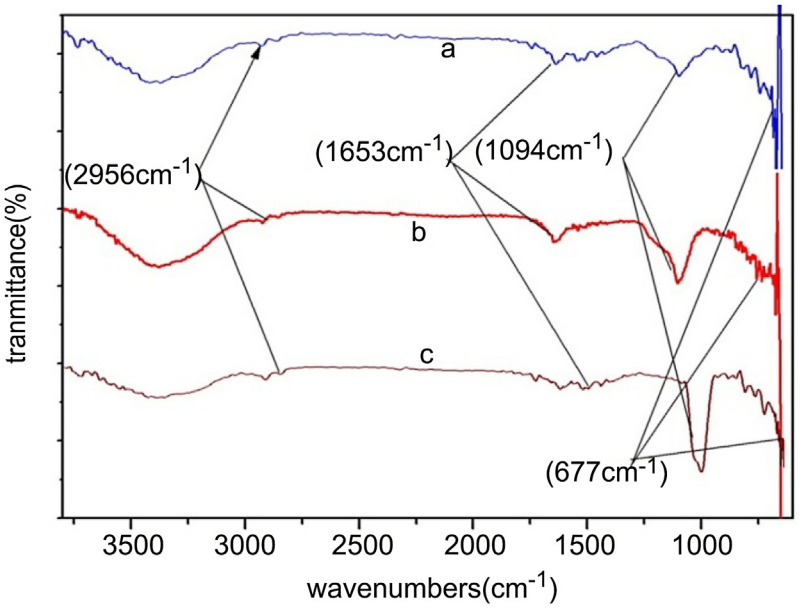

Fig. 3. FT-IR spectrum of α-Fe_2O_3@SiO_2 NPs for different solvents (a) Methanol (b) Ethanol and (c) Isopropanol.

respectively, which was taken at 20 kV accelerating voltage. The SEM images showed that the silica-coated iron oxide nanoparticles were spherical in nature, heterogeneous, small and had an average size of about 118 nm for the solvent methanol. For ethanol the resultant particles were more uniform, spherical, homogeneous and had average size of about 185 nm. On the other hand for isopropanol the particles were spherical, heterogeneous, in large cluster and had average size about 657 nm. From SEM pictures it was analyzed that the alcohols have a great influence on the morphology of the silica coated iron oxide nanoparticles. Difference in the particle size depends on hydrolysis rate of TEOS, molecular weight, polarity of solvent chosen and the dielectric constant of the medium [41].

Rates of the hydrolysis reaction strongly depend on polarity, molecular weight and diffusivity of TEOS in alcohol. The diffusivity of TEOS in the solvent, related to

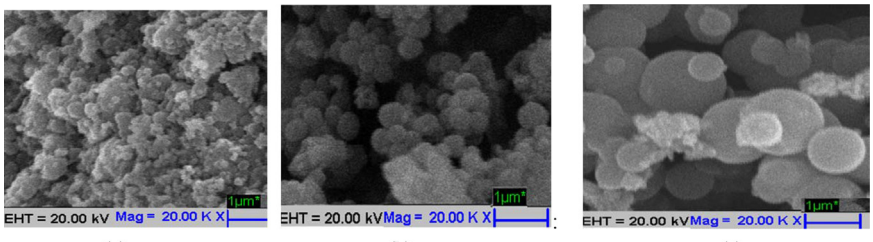

Fig. 4. SEM images of α-Fe_2O_3@SiO_2 NPs prepared by (a) Methanol (b) Ethanol and (c) Isopropanol.

http://dx.doi.org/10.1016/j.heliyon.2017.e00253

its viscosity, decreases with increasing molecular weight of the solvent. In primary alcohols, hydrolysis rate and average particle size increased with molecular weight except methanol, while in secondary alcohols, lower hydrolysis rate and larger particle size was obtained. Among the chosen solvents methanol had highest hydrolysis rate and the smallest particle size due to strong polarity. This exceptional behaviour of methanol is mainly attributed to transesterification. The exchange rate increases when the steric hindrance of alkoxy group decreases. Highest rate of alkoxy exchange of TEOS is found in methanol [42, 43]. The varying sizes of the particles are directly correlated with the dielectric constant of the medium. The nanoparticles prepared using methanol as a solvent were found smallest in size due to the highest dielectric constant of methanol medium [44]. Silica nanoparticles prepared by ethanol were homogeneous as compared to other solvents due to simultaneous uniform formation of all the nuclei and subsequent growth under the same conditions. Nucleation occurs when the concentration reaches the minimum saturation required to generate the critical free energy [45]. Once nuclei are formed, growth occurs simultaneously, nucleation and growth are inseparable processes having different speeds.

3.2. Magnetic properties

3.2.1. (a) Magnetic measurements of α-Fe_2O_3 and α-Fe_2O_3@SiO_2 nanoparticles

The magnetic properties of the prepared nanoparticles were examined by vibrating sample magnetometer (VSM). The *M-H* curve for α-Fe_2O_3 and of α-Fe_2O_3 @ SiO_2 nanoparticles using different solvents methanol, ethanol and isopropanol at temperature 302.5 K is presented in Fig. 5. The curve showed that both hematite and α-Fe_2O_3 @ SiO_2 nanoparticles exhibited a small magnetic hysteresis and typically weak ferromagnetic behaviour. Magnetic properties of a material are influenced by different factors like size, structure, crystallinity and crystal defects etc. It has been observed that type of solvent used for preparation strongly affects the magnetization but the magnetic behaviour remains unchanged. Saturation magnetization, remanent magnetization and coercivity of all the samples are reported in Table 2.

The saturation magnetization and residual induction of α-Fe_2O_3@SiO_2 nanoparticles were found to be lower than those of uncoated α-Fe_2O_3 nanoparticles. The change in values is correlated with the change of magnetic particle sizes and iron ion concentration [20]. When silica is bonded on the surface of α-Fe_2O_3 nanoparticles, Si-O-Fe bond has been formed. The magnetic moment of iron ions on the surface of α-Fe_2O_3 nanoparticles disappeared through the Si-O-Fe connection and as a result, magnetism decreased. The result shows that the saturation magnetization decreases from 0.25 to 0.127, 0.0801 and 0.076 emu g^{-1}

http://dx.doi.org/10.1016/j.heliyon.2017.e00253

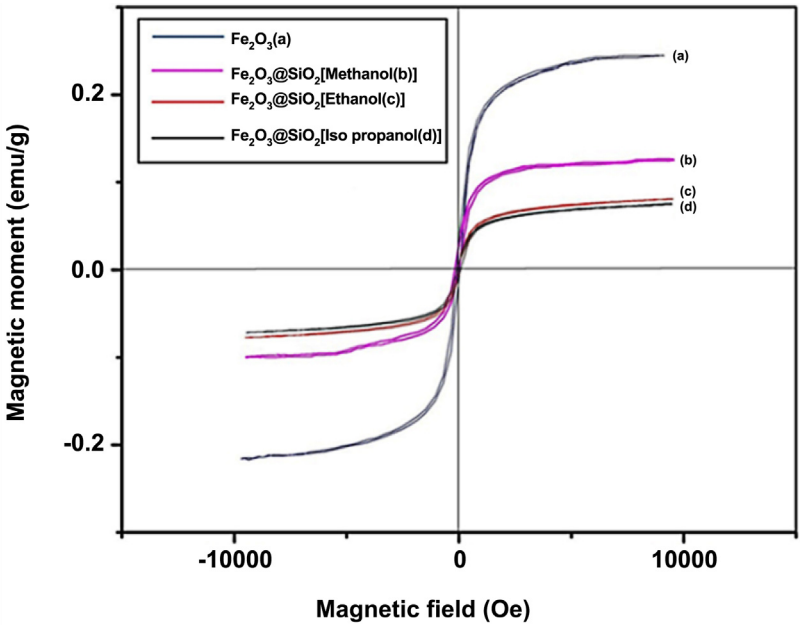

Fig. 5. M-H curve of α-Fe_2O_3 and of α-Fe_2O_3 @ SiO_2 nanoparticles at 302.5 K using different solvents.

and remanent magnetization also decreases from 0.048 to 0.029, 0.0088 and 0.0079 emu g^{-1} for silica coated iron oxide nanoparticles obtained by using solvent methanol, ethanol & isopropanol, respectively. This is due to increase in shell thickness from methanol to ethanol to isopropanol. Silica nanoparticles prepared by solvent isopropanol were largest in size as compared to other solvents, so the saturation magnetization was lowest for these α-Fe_2O_3@SiO_2 nanoparticles due to large volume of amorphous silica phase [46]. Unlike the saturation magnetization and residual induction, the coercivity of α-Fe_2O_3 nanoparticles increased after silica coating. The change in the direction of magnetic moment of iron ions became difficult near the surface of α-Fe_2O_3 nanoparticles due to Si-O-Fe connection generated by silica coating. So, silica coating protects the magnetic particles from possible decomposition induced by surrounding environment, prevents further

Table 2. Magnetic parameters obtain from VSM for pure α-Fe_2O_3 & α-Fe_2O_3 @ SiO_2 core- shell nanoparticles.

NPs	Saturation magnetization (M_s)	Remanent magnetizations (M_r)	Coercivity (H_c)
α-Fe_2O_3	0.25 emu g^{-1}	0.048 emu g^{-1}	54.08 Oe
α-Fe_2O_3 @ SiO_2 (methanol)	0.127 emu g^{-1}	0.029 emu g^{-1}	75.45 Oe
α-Fe_2O_3 @ SiO_2 (ethanol)	0.0801 emu g^{-1}	0.0088 emu g^{-1}	85.83 Oe
α-Fe_2O_3 @ SiO_2 (isopropanol)	0.076 emu g^{-1}	0.0079 emu g^{-1}	91.313 Oe

http://dx.doi.org/10.1016/j.heliyon.2017.e00253

aggregation and reduces inter particle magnetic cross talk retaining the magnetic property of each particle intact.

3.3. Dielectric properties

3.3.1. (a) Dielectric properties of pure SiO_2 nanoparticles

The method of preparation, chemical composition and microstructure determines the dielectric properties of silica. At room temperature the values of the dielectric constant and the dielectric loss of the pure silica samples were analyzed within a stipulated frequency range (1KHz–1 MHz).

Fig. 6(a and b) show the variation of the dielectric constant and dielectric loss as a function of frequency for pure silica nanoparticles in solvents methanol, ethanol and iospropanol respectively. For all the silica samples, a decreasing trend in dielectric constant and dielectric loss has been observed with increasing frequency at room temperature.

At lower frequencies, this decrement is rapid, whereas, at higher frequencies it is slower and much stable. Interfacial polarization can be experienced by silica nanoparticles at low frequency region, because they are considered as hetrogeneous materials. At high frequency, reduction in the values of dielectric constant can be explained by hopping mechanism under the influence of alternating current. The frequency of hopping between ions lags behind the frequency of applied field.

On studying and analyzing it has been observed that the dielectric loss strongly depends on the frequency of the applied field, which is similar to that of the dielectric constant. Due to the dielectric polarization, space charge and rotation, high energy loss is observed in the low frequency range. The dipole relaxation also defines the variation of dielectric loss with the frequency. Dipoles switch their

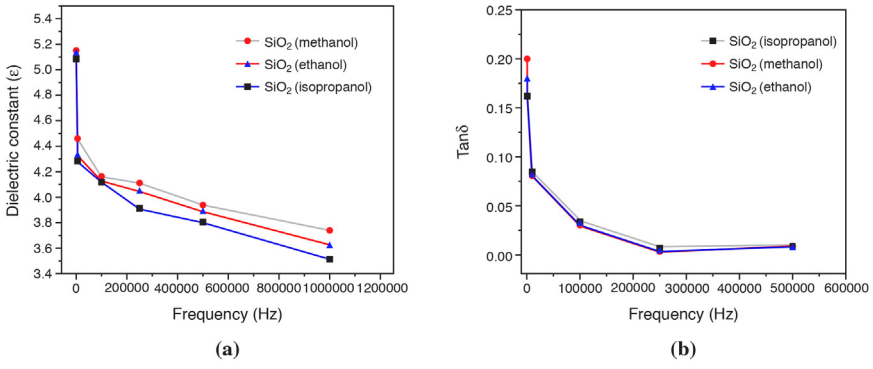

Fig. 6. (a) Dielectric Constant and (b) Dielectric Loss variation with Frequency at room Temperature for pure SiO2.

http://dx.doi.org/10.1016/j.heliyon.2017.e00253

alignment with the changing field at lower frequency, whereas, with the increase in frequency the rotation of dipole is less reducing their contribution to the changing polarization field. The dielectric results showed that there is slight difference in the value of dielectric constant and loss in silica nanoparticles prepared by various solvents, which might be due to change in size of prepared particles. The increase in the particle size from methanol to ethanol to isopropanol as verified by the SEM analysis might have reduced the electric dipole inside the samples and consequently dielectric constant decreased.

3.3.2. (b) Dielectric properties of α-Fe_2O_3@SiO_2 nanoparticles

The dielectric constant and the dielectric loss of α-Fe_2O_3@SiO_2 core shell nanoparticles using solvent methanol were also studied at room temperatures in the same frequency region. It was observed from Fig. 7(a and b) that the dielectric constant and dielectric loss showed the same decreasing trend with increasing frequency like pure silica nanoparticles.

From the above results, it can be concluded that silica coated iron oxide nanoparticles, show decrement in the value of dielectric constant (from 5.2 to 3.2) and increment in dielectric loss (from .2 to .27) in comparison to pure silica nanoparticles due to some contribution in conductivity by metallic iron nanoparticles core. The low dielectric loss with high frequency for a given sample suggested that the sample had good optical quality with lesser defects and this parameter plays a vital role in nonlinear optical materials. Low dielectric loss suggested that low charges induced by the external field were dissipated. The above findings suggest that the dielectric behaviour of silica remains same for all the types of solvent used, but the values of dielectric constant and loss varies with solvent variation, due to morphological change in the prepared sample. The results show that silica can be used very efficiently as a protective layer over the iron-

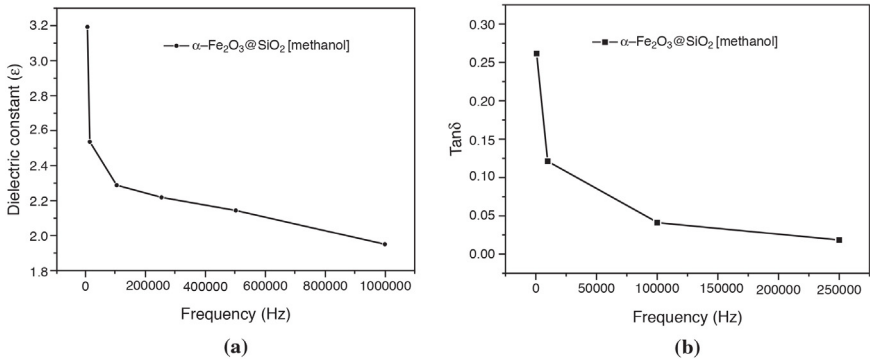

Fig. 7. (a) Dielectric Constant and (b) Dielectric Loss variation with Frequency at room temperature for α-Fe_2O_3@SiO_2.

http://dx.doi.org/10.1016/j.heliyon.2017.e00253

oxide nanoparticles to shield their magnetic behaviour and preventing them from conducting charges.

4. Conclusion

Surface coating and functionalization of iron oxide nanoparticles not only stabilizes the nanoparticles but also provided the special functional group for attaching the biological molecules of interest. The size of the obtained silica-coated magnetic nanoparticles increases with decrease in polarity of alcohol from methanol to ethanol to isopropanol. Magnetic study revealed that the weak ferromagnetic behaviour of uncoated α-Fe_2O_3 remains the same even after coating with silica. However, magnetic parameters of core α-Fe_2O_3 nanoparticles after coating with silica varied, due to slight decrement in the size of the core nanoparticles and formation of Fe-O-Si bonds at the surface. The higher value of coercivity of silica-coated iron oxide nanoparticles shows that the stability of α-Fe_2O_3@SiO_2 nanoparticles was more as compared to their parent α-Fe_2O_3 nanoparticles. Dielectric study shows that the prepared particles show better insulating behaviour in all the solvents. Size variation owing to the types of solvent used, endorsed slight change in the value of dielectric constant. Therefore, highly insulated silica nanoparticles provide better stability and thermal insulation to core iron oxide nanoparticles.

Declarations

Author contribution statement

Deepika P Joshi: Conceived and designed the experiments; Performed the experiments; Analyzed and interpreted the data; Contributed reagents, materials, analysis tools or data; Wrote the paper.

Geeta Pant: Performed the experiments; Analyzed and interpreted the data.

Neha Arora: Analyzed and interpreted the data; Wrote the paper.

Seema Nainwal: Contributed reagents, materials, analysis tools or data.

Funding statement

This research did not receive any specific grant from funding agencies in the public, commercial, or not-for-profit sectors.

Competing interest statement

The authors declare no conflict of interest.

http://dx.doi.org/10.1016/j.heliyon.2017.e00253

Additional information

No additional information is available for this paper.

References

[1] J.B. Jackson, N.J. Halas, Silver nanoshells: Variations in Morphologies and Optical Properties, J. Phys. Chem. B 105 (2001) 2743–2746.

[2] K.L. Kelly, E. Coronado, L.L. Zhao, G.C. Schatz, The Optical Properties of Metal Nanoparticles: The Influence of Size Shape, and Dielectric Environment, J. Phys. Chem. B 107 (2003) 668–677.

[3] G. Jinhao, G. Hongwei, X. Bing, Multifunctional Magnetic Nanoparticles: Design, Synthesis, and Biomedical Applications, Acc. Chem. Res. 42 (2009) 1097–1107.

[4] A. Manikandan, L.J. Kennedy, J.J. Vijaya, Structural, optical and magnetic properties of porous α-Fe_2O_3 nanostructures prepared by rapid combustion method, J. Nanosci. Nanotechnol. 13 (2013) 2986–2992.

[5] K. Chinnaraj, A. Manikandan, P. Ramu, S.A. Antony, P. Neeraja, Comparative study of microwave and sol-gel assisted combustion methods of Fe_3O_4 nanostructures: Structural, morphological, optical, magnetic and catalytic properties, J. Supercond. Nov. Magn. 28 (2015) 179–190.

[6] F. Ozel, H. Kockar, O. Karaagac, Growth of Iron Oxide Nanoparticles by Hydrothermal Process: Effect of reaction parameters on the nanoparticle size, J. Supercond. Nov. Magn. 28 (2015) 823–829.

[7] O. Karaagac, H. Kockar, T. Tanrisever, Properties of iron oxide nanoparticles synthesized at different temperatures, J. Supercond. Nov. Magn. 24 (2011) 675–678.

[8] S. Beyaz, F. Ozel, H. Kockar, T. Tanrisever, Use of Triethylene Glycol Monobutyl Ether on Synthesis of Iron Oxide Nanoparticles, J. Magn. Magn. Mater. 361 (2014) 249–251.

[9] A. Manikandan, A. Saravanan, S.A. Antony, M. Bououdina, One-pot low temperature synthesis and characterization studies of nanocrystalline α-Fe_2O_3 based dye sensitized solar cells, J. Nanosci. Nanotechnol. 15 (2015) 4358–4366.

[10] A. Manikandan, M. Durka, K. Seevakan, S.A. Antony, A novel one-pot combustion synthesis and opto-magnetic properties of magnetically separable spinel MnxMg1-xFe_2O_4 (0. 0 ≤ x ≤ 0.5) nano-photocatalysts, J. Supercond. Nov. Magn. 28 (2015) 1405–1416.

 http://dx.doi.org/10.1016/j.heliyon.2017.e00253

[11] V.M. Teresita, A. Manikandan, B.A. Josephine, S. Sujatha, S.A. Antony, Electro-magnetic properties and humidity sensing studies of magnetically recoverable $LaMg_xFe_{1-x}O_{3-\delta}$ perovskites nano-photocatalysts by sol-gel route, J. Supercond. Nov. Magn. 29 (2016) 1691–1701.

[12] E. Hema, A. Manikandan, P. Karthika, M. Durka, S.A. Antony, B.R. Venkatraman, A novel synthesis of $Zn^{2+?}$doped $CoFe_2O_4$ spinel nanoparticles: Structural, morphological, opto-magnetic and catalytic properties, J. Supercond. Nov. Magn. 28 (8) (2015) 2539–2552.

[13] V. Umapathy, A. Manikandan, P. Ramu, S.A. Antony, P. Neeraja, Synthesis and characterizations of $Fe_2(MoO_4)_3$ nano-photocatalysts by simple sol-gel method, J. Nanosci. Nanotechnol. 16 (2016) 987–993.

[14] S. Jayasree, A. Manikandan, S.A. Antony, A.M.U. Mohideen, C. Barathiraja, Magneto-optical and catalytic properties of recyclable spinel NiAl2O4 nanostructures using facile combustion methods, J. Supercond. Nov. Magn. 29 (2016) 253–263.

[15] A.P. Subramanian, S.K. Jaganathan, A. Manikandan, K.N. Pandiaraj, N. Gomathi, E. Supriyanto, Recent trends in nano based drug delivery systems for efficient delivery of phytochemicals in chemotherapy, RSC Adv. 6 (2016) 48294–48314.

[16] V. Muthuvignesh, V.J. Reddy, S. Ramakrishna, S. Ray, A. Ismail, M. Mandal, A. Manikandan, S. Seal, S.K. Jaganathan, Electrospinning applications from diagnosis to treatment of diabetes, RSC Adv. 6 (2016) 83638–83655.

[17] J.A. Mary, A. Manikandan, L.J. Kennedy, M. Bououdina, R. Sundaram, J.J. Vijaya, Structure and magnetic properties of Cu-Ni alloy nanoparticles prepared by rapid microwave combustion method, Trans. Nonferrous Met. Soc. China 24 (2014) 1467–1473.

[18] V. Muthuvignesh, S.K. Jaganathan, A. Manikandan, Nanomaterials as a game changer in the management and treatment of diabetic foot ulcers, RSC Adv. 6 (2016) 114859–114878.

[19] J.K. Oha, J.M. Park, Iron oxide-based superparamagnetic polymeric nanomaterials: Design, preparation, and biomedical application, Prog. Polym. Sci. 36 (2011) 168–189.

[20] O. Karaagac, H. Kockar, A simple way to obtain high saturation magnetization for superparamagnetic iron oxide nanoparticles synthesized in air atmosphere: Optimization by experimental design, J. Magn. Magn. Mater. 409 (2016) 116–123.

 http://dx.doi.org/10.1016/j.heliyon.2017.e00253

[21] F. Ozel, H. Kockar, S. Beyaz, O. Karaagac, T. Tanrisever, Superparamagnetic iron oxide nanoparticles: effect of iron oleate precursors obtained with a simple way, J. Mater. Sci. Mater. Electron. 24 (8) (2013) 3073–3080.

[22] S. Beyaz, T. Tanrisever, H. Kockar, V. Butun, Superparamagnetic latex synthesized by a new route of emulsifier-free polymerization, J. Appl. Polym. Sci. 121 (2011) 2264–2272.

[23] O. Karaagac, H. Kockar, Effect of Synthesis Parameters on the Properties of Superparamagnetic Iron Oxide Nanoparticles, J. Supercond. Nov. Magn. 25 (2012) 2777–2781.

[24] M. Chirita, I. Grozescu, Fe_2O_3–nanoparticles, physical properties and their photochemical and photoelectron chemical applications, Chemical Bulletin of Politehnica University 54 (2009) 1–8.

[25] X. Zhang, Y. Niu, Y. Li, X. Hou, Y. Wang, R. Bai, J. Zhao, Synthesis, optical and magnetic properties of α-Fe_2O_3 nanoparticles with various shapes, Mater. Lett. 99 (2013) 111–114.

[26] F. Bodker, M.F. Hansen, Magnetic properties of hematite nanoparticles, Phys. Rev. B 61 (2000) 1626–1638.

[27] P. Allia, G. Barrera, B. Bonelli, F.S. Freyria, P. Tiberto, Magnetic properties of pure and Eu-doped hematite nanoparticles, J. Nanopart. Res. 15 (2013).

[28] Z. Donglin, Z. Hongsheng, Z. Wancheng, Dielectric properties of nano Si═C═N composite powder and nano SiC powder at high frequencies, Physica E 9 (2001) 679–685.

[29] M.N. Ashiq, M.J. Iqbal, I.H. Gul, Effect of Al–Cr doping on the structural, magnetic and dielectric properties of strontium hexaferrite nanomaterials, J. Magn. Magn. Mater. 323 (2011) 259–263.

[30] L. Zhimin, Z. Wancheng, S. Xiaolei, H. Yunxia, L. Guifang, W. Yupen, Dielectric Property of Aluminum-Doped SiC Powder by Solid-State Reaction, J. Am. Ceram. Soc. 92 (2009) 2116–2118.

[31] M. Jose, V. Sumithra, S. Rajan, Prajeshkumar, J. Mathew, Dielectric properties of nanocrystalline ZnS, SB Academic Review XVII: No.1 and 2 (2010) 93–100.

[32] R. Stanley, A. Nesaraj, Effect of surfactants on the wet chemical synthesis of silica nanoparticles, Int. J. Appl. Sci. Eng. 12 (2014) 9–21.

[33] I. Rahman, V. Padavettan, Synthesis of silica nanoparticles by sol-gel:size-dependent properties, surface modification, and applications in silica-polymer nanocomposites—a review, J. Nanomater (2012) 1–15.

 http://dx.doi.org/10.1016/j.heliyon.2017.e00253

[34] S. Yu, G.M. Chow, Carboxyl group (-CO2H) functionalized ferrimagnetic iron oxide nanoparticles for potential bio-applications, J. Mater. Chem. 14 (2004) 2781–2786.

[35] I.I. Lim, P.N. Njoki, H.Y. Park, X. Wang, L. Wang, D. Mott, C.J. Zhong, Gold and magnetic oxide/gold core/shell nanoparticles as bio-functional nanoprobes, Nanotechnology 19 (2008) 305102–305112.

[36] L. Wang, H.Y. Park, I. Stephanie, I. Lim, M.J. Schadt, D. Mott, J. Luo, X. Wang, C.J. Zhong, Core@ shell nanomaterials: gold-coated magnetic oxide nanoparticles, J. Mater. Chem. 18 (23) (2008) 2629–2635.

[37] S. Shaker, S. Zafarian, C.H. Chakra, K.V. Rao, Preparation and Characterisation of Magnetite Nanoparticles by Sol-gel Method for Water Treatment, International Journal of Innovative Research in Science Engineering and Technology 2 (7) (2013) 2969–2973.

[38] A. Sharafi, N. Farhadyar, Preparation of Fe_3O_4@SiO_2 Nanostructures via Inverse Micelle Method and Study of Their Magnetic Properties for Biological Applications, Int. J. Bio-Inorg. Hybrid Nanomater. 2 (2013) 309–313.

[39] M.A. Karakassides, D. Gournis, D. Petridis, An infrared reflectance study of Si-O vibrations in thermally treated alkali saturated montmorillonites, Clay Miner. 34 (1999) 429–438.

[40] L.J. Preston, M.R.M. Izawa, N.R. Banerjee, Infrared Spectroscopic Characterization of Organic Matter Associated with Microbial Bioalteration Textures in Basaltic Glass, Astrobiology 11 (2011) 585–599.

[41] F. Dang, N. Enomoto, J. Hojo, K. Enpuku, Sonochemical Coating of Magnetite Nanoparticles with Silica, Ultrason. Sonochem. 17 (2010) 193–199.

[42] B.W. Peace, K.G. Mayhan, J.F. Montle, Polymers from the hydrolysis of tetraethoxysilane, Polymer 14 (9) (1973) 420–422.

[43] I. Hasegawa, S. Sakka, Transesterification reaction of tetraethoxysilane and butyl alcohols, Bull. Chem. Soc. Jpn. 61 (11) (1988) 4087–4092.

[44] T.K. Singh, C.L. Jain, S.K. Sharma, S.S. Singh, Preparation of dispersed silica by hydrolysis of tetraethylorthosilicate, Indian J. Eng. Mater. Sci. 6 (1999) 349–351.

[45] M. Haruta, B. Delmon, Preparation of homodispersed solids, J. Chim. Phys. Physico-Chim. Biol. 83 (1986) 859.

 http://dx.doi.org/10.1016/j.heliyon.2017.e00253

[46] Ji-Hun Yu, Chang-Woo Lee, Sung-Soon Im, Jai-Sung Lee, Structure and magnetic properties of SiO_2 coated Fe_2 O_3 nanoparticles synthesized by chemical vapor condensation process, Rev. Adv. Mater. Sci. 4 (2003) 55–59.

 http://dx.doi.org/10.1016/j.heliyon.2017.e00253